

## SEISMIC RESPONSE OF BALLOON TYPE CLT SHEAR WALLS

Zhiyong Chen<sup>1</sup>, Marjan Popovski<sup>2</sup>

**ABSTRACT:** Balloon-type mass timber shear walls are one of the most efficient structural systems to resist lateral loads induced by earthquakes or high winds. This system, however, is not included in the 2020 National Building Code of Canada and has no design guidelines in the 2019 Canadian Standard for Engineering Design in Wood, so it is out of reach of most designers. A multi-year research project has been initiated at FPInnovations to quantify the system performance and develop the necessary technical information to codify balloon-type mass timber shear walls. This paper presents the initial results of a study on the seismic response of balloon-type CLT shear walls. A mechanics-based analytical model was updated to predict the CLT panel resistance, in addition to predicting the deflection and resistance of balloon type CLT shear walls. The influence of specific key parameters such as wall length and thickness, aspect ratio, vertical loads, and vertical joints, on the structural performance of this wall system under lateral loads was investigated using the updated model. The results of this study will give a valuable insight into the seismic performance of balloon type CLT shear walls.

**KEYWORDS:** Mass timber, CLT, balloon walls, tall wood construction, seismic response, numerical model

### 1 INTRODUCTION

Balloon-type mass timber shear walls (Figure 1) are one of the most efficient structural systems to resist lateral loads induced by earthquakes or high winds. They allow use of longer mass timber panels, reduction of number of connections, and prevention of the accumulated compression perpendicular to grain in floor panels [1]. This system, however, is not included in the 2020 National Building Code of Canada and has no design guidelines in the 2019 Canadian Standard for Engineering Design in Wood, so it is out of reach of most designers.



*Figure 1: Example of a balloon wall in CLT construction*

Most of the research on CLT as a lateral load resisting system so far has been conducted on platform-type construction [2]. A multi-year research project has been initiated at FPInnovations to quantify the system

performance and develop the design information to codify balloon-type mass timber shear walls [3]. This paper presents the initial results of the study related to the seismic response of balloon-type CLT shear walls. A mechanics-based analytical model [1] was updated to predict the CLT panel resistance, in addition to predicting the deflection and resistance of these types of CLT shear walls. The influence of wall length and thickness, wall aspect ratio, vertical loads, and vertical joint properties on the structural performance of this wall system under seismic loads was investigated using the developed model.

### 2 ANALYTICAL MODELS

#### 2.1 DEVELOPED MODELS

Two analytical models (rigid- and elastic-base models) were developed and verified at FPInnovations to predict the resistance and deflection of balloon-type CLT shear walls [4]. Single- and coupled panel balloon-type CLT walls (Figure 2) were considered by the developed models [1]. The seismic actions on these walls create a base shear force and overturning moment(s). As illustrated in Figure 2, the vertical uplift forces are taken by hold-downs at both ends of the wall, while the shear forces are taken by shear connectors, shear keys, or both. The vertical joints between the panels are not only used to connect the panels in the coupled walls, but also add to the energy dissipation properties of the system. Using the capacity design methodology for seismic lateral loads, the capacity of the wall system is governed solely by the capacity of the connections. The CLT panels are designed to exhibit elastic in-plane deformations, while the connections provide all the ductility and energy dissipation [5, 6].

<sup>1</sup> Zhiyong Chen, FPInnovations, Canada,  
zhiyong.chen@fpinnovations.ca

<sup>2</sup> Marjan Popovski, FPInnovations, Canada,  
marjan.popovski@fpinnovations.ca

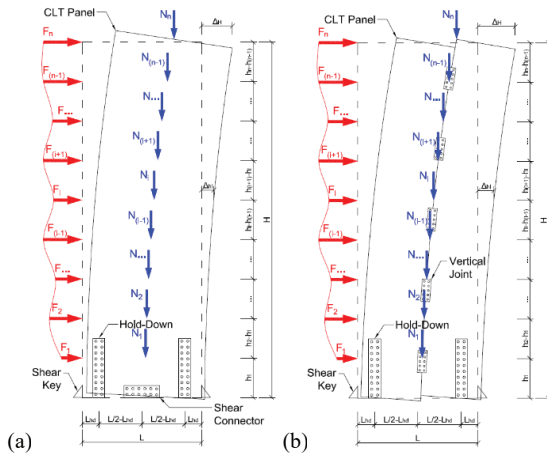


**Figure 2:** (a) Single and (b) coupled wall model. Note:  $F_i$  and  $N_i$  represent the lateral load and the vertical load on the wall at a height level  $i$ , respectively [kN];  $h_i$  represents the height level of the lateral and vertical load [m]; the deflection of the wall at (level  $h_n = H$ ) and at any level  $i$  is designated as  $\Delta H$  and  $\Delta_{hi}$ , respectively [mm];  $n$  indicates the number of load levels.

The total lateral deflection of a single-panel balloon-type CLT shear wall at any height level  $i$ ,  $\Delta_{hi}$ , is comprised of four deflection components: wall bending  $\Delta_{hi,b}$ , wall shear  $\Delta_{hi,s}$ , rotation (anchorage deformation)  $\Delta_{hi,rot}$ , and sliding  $\Delta_{hi,slid}$  (Figure 3a to 3d). In case of walls with multiple panels an additional component  $\Delta_{hi,slp}$  (Figure 3e) that represents the slip between the panels, needs to be added. Thus, the total deflection can be calculated using Eq. (1).

$$\Delta_{hi} = \Delta_{hi,b} + \Delta_{hi,s} + \Delta_{hi,rot} + \Delta_{hi,slid} + \Delta_{hi,slp} \quad (1)$$

The lateral resistance of the system is governed by the strength of the hold-downs, shear connector(s), wood in contact with shear keys, and vertical joints, if present, using three failure scenarios: (a) when shear failure occurs in the bottom connections where the hold-downs and shear connector yield horizontally, and the wood in contact with the shear key at one end crushes successively under base shear; (b) when overturning occurs in single-panel walls where the hold-down at one end yields vertically; and (c) when overturning occurs in coupled walls where the vertical joints yield first followed by yielding of hold-down at one end. The actual resistance can be taken as the minimum resistance derived from the three scenarios.

The balloon-type shear wall is a statically indeterminate system where the connections resist the loads following deformation coordination principle. The deflection and resistance of the wall system can be derived by solving the nonlinear equations of the developed analytical models using the trial-and-error method. Detailed derivation of the deformation components and resistances in different scenarios is provided in Chen and Popovski [1].

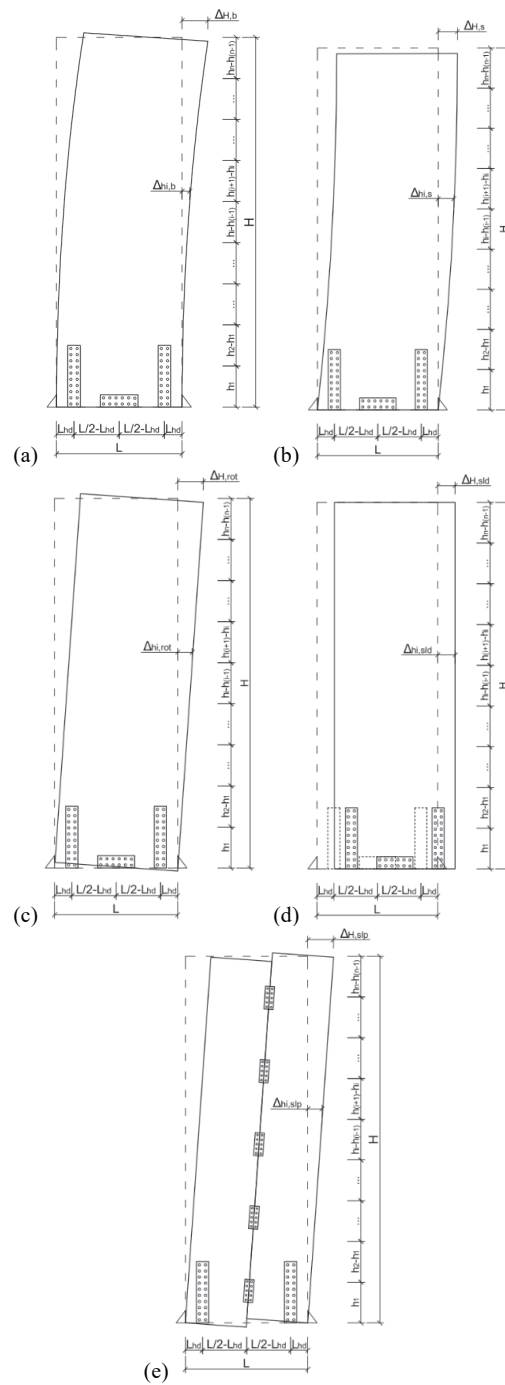


**Figure 3:** Lateral deflection components of balloon-type walls: (a) bending; (b) shear; (c) rotation; (d) sliding; and (e) slip

Generally, the CLT panels in balloon wall system when subjected to in-plane lateral loads present a complex stress state and many failure modes need to be considered in the design [7]. Therefore, the developed elastic-base model was updated in this study to predict the CLT panel resistance to support the capacity design of the balloon-type CLT shear walls.

## 2.2 PANEL RESISTANCE

CLT panels considered in this study have all longitudinal layer with equal thickness and equal width of the boards in the layers. It is assumed that the resistance of CLT panels is governed by bending and shear failure (gross shear, net shear, rolling shear and torsion). It is also assumed that reinforcing solutions are present in areas where some stress concentration is to be expected, e.g., around openings, bottom of the panels, and others, so that the failure does not occur in the panel.

A balloon-type CLT shear wall acts like a vertical cantilever beam in which the wall panels generally behave elastically. The normal stress distribution due to bending in the cross section of the CLT panel is illustrated in Figure 4. Accordingly, the maximum bending stress,  $\sigma_{max}$ , at the bottom for a balloon-type shear wall under a number of lateral loads at different height levels can be calculated using Eq.(2) that is derived using structural mechanics based on a beam theory.

$$\sigma_{max} = \frac{LE_{mean}}{2(EI)_{eff}} \sum_{j=1}^n F_j h_j \quad (2)$$

where  $E_{mean}$  is the mean modulus of elasticity [N/mm<sup>2</sup>] of the longitudinal layers (the horizontal layers in Figure 4) of the CLT panel;  $(EI)_{eff}$  is the effective bending stiffness [N·mm<sup>2</sup>] of the CLT panel which can be calculated using the simplified design method [8], or using the k method (composite theory) provided by Blass and Fellmoser [9].

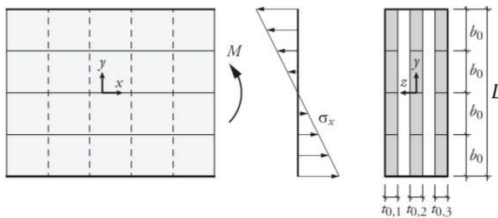


Figure 4. Illustration of normal stress distribution due to bending [7]

The calculated maximum stress should not be larger than the bending strength  $f_b$  of the CLT panel specified in the material design standards or product manuals. Therefore, the maximum base shear  $V_b$  can be calculated using Equation (3).

$$V_b = \frac{2f_b(EI)_{eff}}{LE_{mean}} \sum_{j=1}^n F_{pattern,j} h_j \quad (3)$$

where  $F_{pattern,j}$  is the normalized lateral load factor for the  $j_{th}$  storey according to the lateral load pattern along the height of the wall. Lateral load  $F_j$  is the product of  $V_b$  and  $F_{pattern,j}$ .

In CLT cantilever beams where adjacent lamellas (boards) within individual layer are not edge-glued, the

thickness is not constant throughout the height of the CLT beam. In cross-sections at unglued joints between neighbouring lamellas, the shear forces can only be transferred by lamellas in the perpendicular direction. Consequently, the shear stresses in these so-called net cross sections are higher than in the gross cross-sections (between unglued joints). The transfer of shear forces between longitudinal and transversal lamellas also causes shear stresses in the crossing areas of orthogonally bonded lamellas. By considering the shear stresses in the lamellas and in the crossing areas, three different failure modes (Figure 5) exist in CLT beams subjected to shear stresses [10].

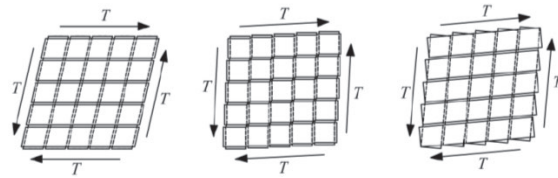


Figure 5. Failure modes I, II and III in CLT-panel subjected to transversal forces in plane direction (from left to right) [10]

Failure mode I is characterised by shear failure parallel to the grain in the gross cross-section of the CLT panels. This failure occurs in sections between unglued joints with  $\tau_l$  equaling to the gross shear strength  $f_{v,gross}$  in longitudinal layers and transversal layers. Therefore, the maximum base shear,  $V_{sl}$ , can be calculated using Equation (4).

$$V_{sl} = \frac{2Lt_{gross}f_{v,gross}}{3} \quad (4)$$

where  $t_{gross}$  is the gross thickness of the CLT panels.

Failure mode II is characterised by shear failure perpendicular to the grain in the net cross-section of the CLT panels. This failure occurs in sections coinciding with unglued joints with shear stresses only in lamellas perpendicular to the joints. The maximum base shears ( $V_{slI,90}$  and  $V_{slI,0}$ ) can be calculated using Eqs. (5) and (6).

$$V_{slI,90} = \frac{2Lt_{net,90}f_v}{3} \quad (5)$$

$$V_{slI,0} = \frac{2Lt_{net,0}f_v}{3} \quad (6)$$

where  $t_{net,90}$  is the total thickness of all perpendicular layers in the CLT panels;  $t_{net,0}$  is the CLT panel net cross-section thickness when considering longitudinal layers only.

Failure mode III is characterised by shear failure within the crossing areas between the orthogonally glued boards (lamellas). This failure mode is caused by torsional and unidirectional shear stresses form the transfer of the shear forces between adjacent layers. The maximum base shear ( $V_{slII}$ ) can be calculated using Equation (7).

$$V_{sIII} = \frac{b_0^2 n_{ca}}{6 \left( \frac{1}{m} + \frac{1}{m^3} \right) \frac{b_0 b_{max}}{f_{tor}} + \frac{6 \left( \frac{1}{m^2} + \frac{1}{m^3} \right) 1.33}{f_s}} \quad (7)$$

where  $n_{ca}$  is the number of crossing areas that longitudinal lamination shares with adjacent transversal laminations;  $m$  is the number of horizontal boards in the CLT beam or  $m = L/b_0$ ;  $q$  is the local compression [kN/m];  $b_{max}$  is the maximum value for the width of either the longitudinal boards ( $b_0$ ) or the transversal boards ( $b_{90}$ ), i.e.,  $b_{max} = \max\{b_0, b_{90}\}$ .

### 3 KEY PARAMETERS AFFECTING STRUCTURAL PERFORMANCE

Using the updated analytical elastic-base model, parametric analyses were conducted to investigate the influence of various key parameters on the structural performance of balloon-type CLT walls. The key parameters that were investigated include (a) CLT panel thickness (number of layers); (b) wall length (panel width); (c) wall aspect ratio; (d) level of vertical loads; and (e) vertical joint properties (coupled walls). The influence of the first four parameters was studied with single-panel shear walls (Figure 2a) under multiple point loads in reversed triangular pattern (Figure 6), while that of the fifth parameter was studied with coupled shear walls (Figure 2b).

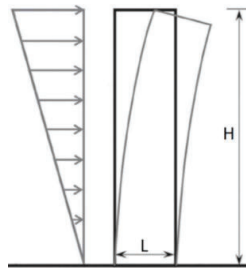


**Figure 6:** Reversed triangular lateral load pattern applied to the wall

The CLT panels and shear connectors were capacity designed; while the hold-downs were designed to yield under lateral loads once the maximum stresses in the panels reach 30% design bending or shear strength, whichever is less, i.e., lateral load level (LLL) = 30%. The distance of hold-downs to the close edge,  $L_{hd}$  (Figure 2), was taken as  $L/20$ .

#### 3.1 WALL LENGTH

The influence of wall length (CLT panel width) was studied on single-panel shear walls with a wall height of 18 m, which is typical for a 6-storey building with a storey height of 3 m. The considered wall lengths,  $L$ , were 2.4 m, 3.0 m, 3.6 m, 4.2 m, 4.8 m, 5.4 m, and 6.0 m. The commonly used 5-, 7-, and 9-ply CLT panels were investigated.

Figures 7 and 8 show the relationship of the wall length to the resistance ( $P_{wall}$ ) and stiffness ( $K_{wall}$ ) of the analysed balloon-type CLT shear walls. The ratios in Figures 7b and 8b were based on the structural performance properties of the shear walls with 3.0 m wall length and a given wall thickness. With an increase in the wall length, the resistance increased linearly, while the stiffness increased nonlinearly. This is because the resistance of all walls was governed by the shear failure, while the deflection was a combination of bending and shear deformation, rotation, and sliding.

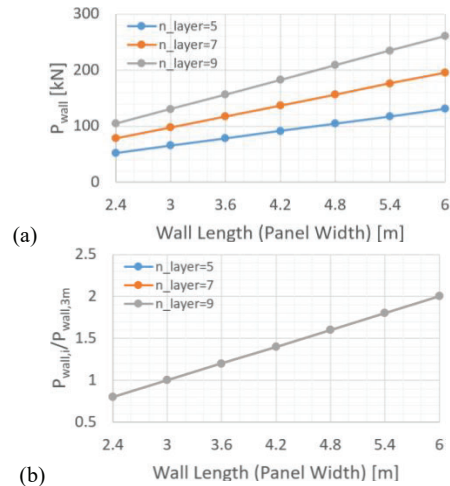


**Figure 7:** Relationship between the wall length and the wall resistance: (a) Absolute values; and (b) Relative values with respect to a 3m long wall

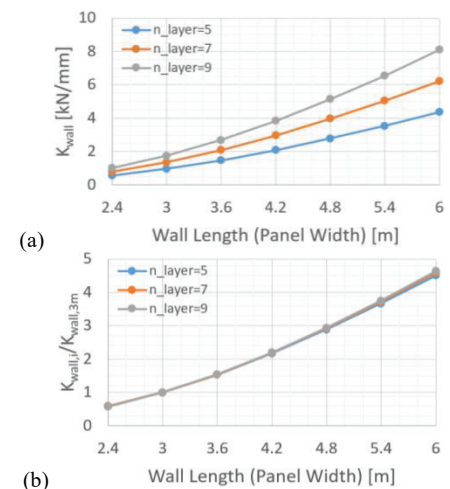


**Figure 8:** Relationship between the wall length and the wall stiffness: (a) Absolute values; and (b) Relative values with respect to 3 m long wall

The relationship between the wall length and the ratio of the compression zone length to the wall length ( $L_c/L$ ) for the analysed balloon-type CLT shear walls is shown in Figure 9. The  $L_c/L$  ratio was constant for all wall lengths

of the same wall thickness. This is because the lateral loads applied on the walls is governed by shear resistance of the panels, which by itself is in linear relationship with the wall length. Thus, the  $L_c/L$  ratio remained constant.

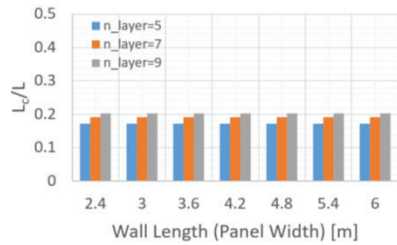


**Figure 9:** Relationship between the wall length and the compression zone length

### 3.2 WALL THICKNESS

The influence of wall thickness can be analysed by comparing the structural performance of the analysed shear walls with different thickness. The thickness depends on the number of layers in the CLT panel (0.175 m for 5-ply, 0.245 m for 7-ply, and 0.315 m for 9-ply panels). The relationship of the wall thickness to the wall resistance and stiffness is shown in Figures 10 and 11. The ratios in Figures 10b and 11b were based on the structural performance properties of walls with 0.175 m thickness (5-ply) for a given wall length. With an increase in wall thickness, the resistance and the stiffness of the shear walls increased linearly. In both, Figure 10b and 11b, the relationships for all wall lengths are identical. All shear walls were governed by shear (type II in transversal laminations) failure of which the resistance and stiffness increase linearly with the number of transversal laminations (i.e., 2, 3, and 4).

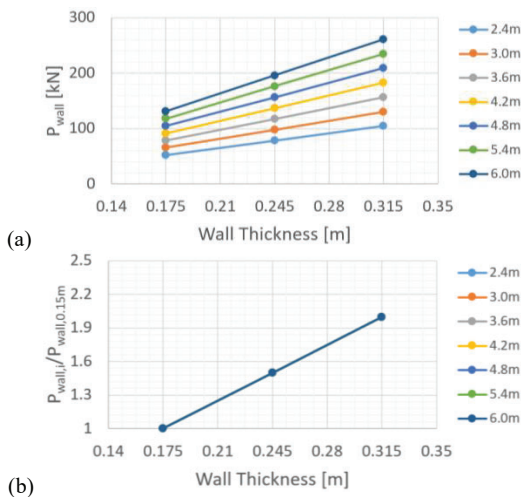


**Figure 10:** Relationship between the wall thickness and the wall resistance: (a) Absolute values; and (b) Relative values with respect to 175 mm thick wall

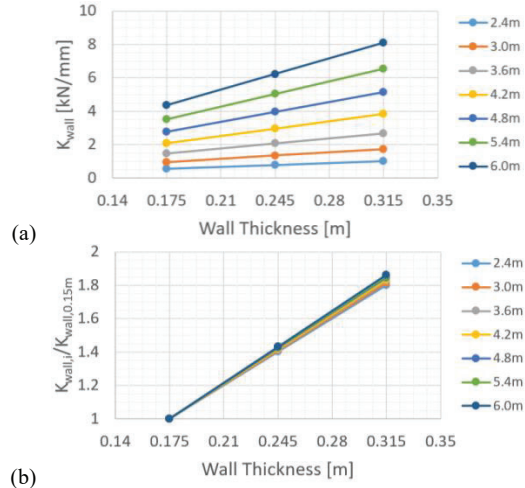


**Figure 11:** Relationship between the wall thickness and the wall stiffness: (a) Absolute values; and (b) Relative values with respect to 175 mm thick wall

The relationship between the wall thickness and the ratio of the compression zone length to the entire wall length ( $L_c/L$ ) for the analysed balloon walls is shown in Figure 12. The ratio  $L_c/L$  increased with an increase in wall thickness.

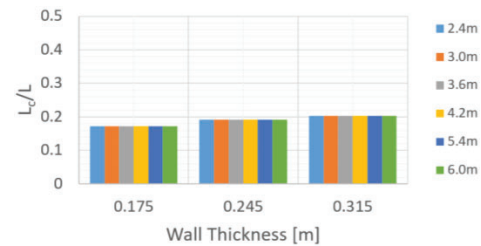


**Figure 12:** Relationship between wall thickness and compression length

### 3.3 WALL ASPECT RATIO

The influence of the wall aspect ratio was studied on 7-ply single-panel shear walls with a wall length of 1.5 m, 3.0 m, and 6.0 m. The considered aspect ratios were 4, 6, 8, 10, and 12. Correspondingly, the wall heights were 6m, 9 m, 12 m, 15 m, and 18 m for 1.5m long shear walls; 12 m, 18 m, 24 m, 30 m, and 36 m for 3.0 m long walls; and 24 m, 36 m, 48 m, 60 m, and 72 m for 6.0 m long walls.

Figures 13 and 14 show the relationship of the wall aspect ratio to wall resistance and stiffness of the analysed balloon walls. The ratios (Figures 13b and 14b) were based on the structural performance properties of the shear walls with the aspect ratio of 4.0 and a given wall length. The resistance kept constant until the aspect ratio of 8.0. Beyond that it decreased in a nonlinear fashion with an increase in the aspect ratio. This is because the shear failure governed the wider walls while bending failure governed the slender walls. The critical aspect

ratio for the change of governing failure mode was around 8.0. The stiffness decreased in a nonlinear fashion with an increase in the aspect ratio. Slender walls showed to have less resistance and be more flexible, compared to wider walls.

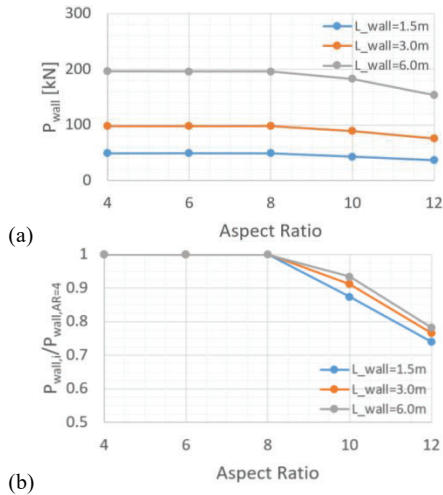


**Figure 13:** Relationship between the aspect ratio and the wall resistance: (a) Absolute values; and (b) Relative values with respect to walls with aspect ratio of 4.0

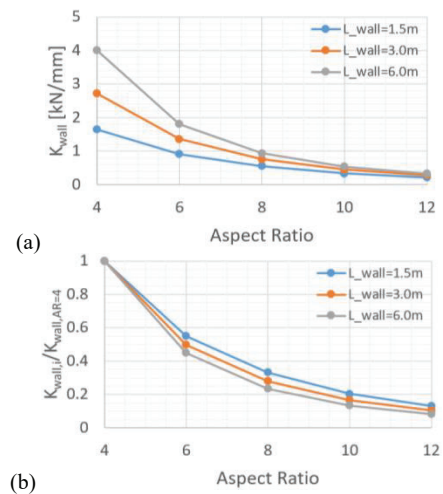


**Figure 14:** Relationship between the aspect ratio and wall stiffness: (a) Absolute values; and (b) Relative values with respect to wall with an aspect ratio of 4.0

The relationship between the wall aspect ratio and the ratio of the compression zone length to the entire wall length ( $L_c/L$ ) for analysed balloon-type CLT shear walls is shown in Figure 15. As can be seen, an increase in wall aspect ratio resulted in a non-linear increase in the  $L_c/L$  ratio until a wall aspect ratio of 8.0, beyond which  $L_c/L$  was constant. For the walls governed by shear failure, where the wall aspect ratio is not larger than 8.0, slender walls needed longer  $L_c$  to resist larger compression under

the same later loads. In walls governed by bending failure, where the wall aspect ratio is over 8.0, a balance was achieved between  $L_c$  and the aspect ratio. A larger wall aspect ratio resulted in an increase in the compression stress at the wall base and thus  $L_c$ ; however, it also reduced the amount lateral load that the wall can carry and thus the compression portion and  $L_c$ .

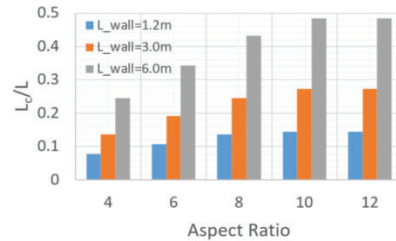


**Figure 15:** Relationship between the wall aspect ratio and the compression zone length for walls designed for the same lateral load

The deflection components of the balloon-type CLT shear walls with different aspect ratios were decoupled and the percentage of each component is shown in Figures 16 to 18. The rotation and bending deflection were the major contributors to the deflection of the walls, while the shear deflection had less contribution. The contribution of sliding was small enough to be ignored. As the wall aspect ratio increased, the walls became slenderer and the contribution of the bending deflection increased and became predominant, while the contribution of rotation and shear deflection decreased. The intersection between the rotation and the bending deformation curves occurred at a lower aspect ratio for longer walls (e.g., 6.0 m) compared to a short wall (e.g., 1.5m). This is due to the fact that the bending deflection is a function of aspect ratio but also of the applied loads. For the same aspect ratio, the higher the loads, the larger the deflection.

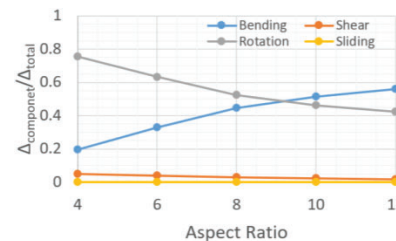


**Figure 16:** Influence of wall aspect ratio on the deflection components in 1.5 m long single-panel walls

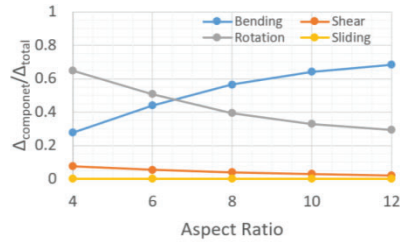


**Figure 17:** Influence of wall aspect ratio on the deflection components in 3.0 m long single-panel walls

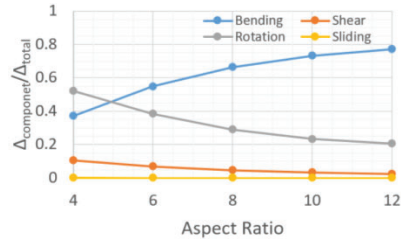
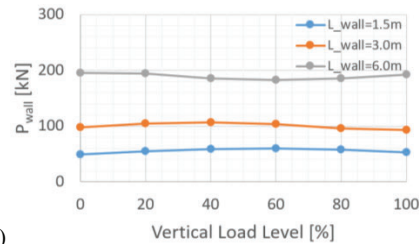


**Figure 18:** Influence of wall aspect ratio on the deflection components in 6.0 m long single-panel walls

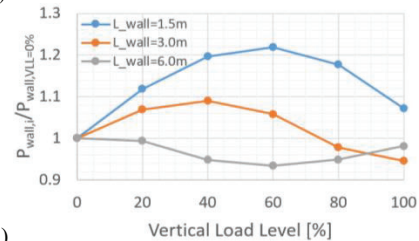
### 3.4 VERTICAL LOADS

Vertical loads applied to the shear walls provide additional overturning resistance to the walls, and as a result, they affect wall's lateral stiffness and resistance. The influence of the vertical loads was studied on 7-ply single-panel shear walls with a wall length of 1.5 m ( $H = 9$  m), 3.0 m ( $H = 18$  m), and 6.0 m ( $H = 36$  m). Six vertical load levels (VLLs), 0%, 20%, 40%, 60%, 80% and 100% of the reference vertical loads, were analysed for each wall length. The reference vertical loads were defined as loads that can counteract the overturning resistance of a wall without vertical loads. Thus, the reference vertical loads were taken as 1200 kN, 2300 kN, and 4300 kN for 1.5 m, 3.0 m, and 6.0 m walls, respectively.

Figures 19 and 20 show the relationship of vertical loads to wall resistance and stiffness of the analysed balloon-type CLT shear walls. The ratios (Figures 19b and 20b) were based on the structural performance properties of the shear walls with the vertical load level of 0% (no vertical loads) and a given wall length. As shown in Figure 19, the resistance of 1.5 m walls increased with an increase in the VLL up to 60% and then started to decrease. The resistance of 3.0 m long walls increased with an increase in the VLL at the beginning, but then very soon after 40% VLL the resistance started to decrease. The resistance of 6.0 m walls decreased with an increase in VLL until VLL reached 60% beyond which the resistance increased with the increases in the VLL. As shown in Figure 20, the stiffness of 1.5 m and 3.0 m long walls increased with an increase in VLL, while the stiffness of 6.0 m walls decreased with an increase in VLL. All these findings indicate that the wall resistance and stiffness were affected by not only the VLL, but also the ratio between compression length and the wall length ( $L_c/L$ , Figure 21).

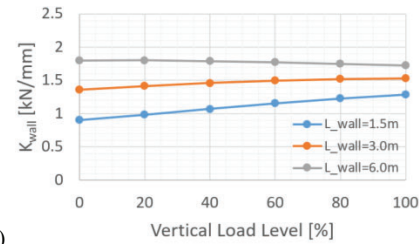


(a)

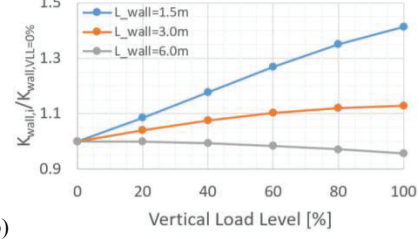


(b)

**Figure 19:** Relationship between VLL and wall resistance: (a) Absolute values; and (b) Relative values with respect to vertical load without vertical load



(a)



(b)

**Figure 20:** Relationship between vertical loads level and compression zone length

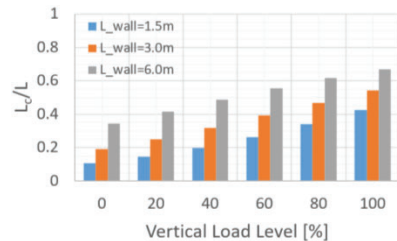


**Figure 21:** Relationship between vertical loads level and compression zone length

The stiffness of the walls increased with an increase in VLL when  $L_c/L$  was less than 0.4 and decreased when  $L_c/L$  was larger than 0.4. The resistance of walls increased with an increase in VLL when  $L_c/L$  was either

less than 0.4 or larger than 0.6, while it decreased with an increase in VLL when  $L_c/L$  was between 0.4 and 0.6. This is because the effect of vertical loads changes from being helpful (increasing the resistance) to detrimental (decreasing the resistance) under lateral loads, when  $L_c/L$  changes from less than 0.4 to larger than 0.6, with the range of 0.4 to 0.6  $L_c/L$  been the transition zone. For cases with large  $L_c/L$  (e.g., over 0.6), the vertical loads provide some kind of prestressing at the wall bottom and thus increase the wall resistance.

### 3.5 VERTICAL JOINTS

The influence of the vertical joints was studied on a 7-ply coupled balloon-type CLT walls with two configurations. Configuration A was a 9 m high coupled wall with 1.5 m panel width (3.0 m total wall length), while Configuration B was 18 m high coupled wall with 3.0 m panel width and a total wall length of 6.0 m. A shear stiffness ratio (SSR) was defined as the ratio of the stiffness of the vertical joints to the shear stiffness of the wall along the height. Seven (7) shear stiffness ratios (SSR) were considered in the investigation: 0.01, 0.1, 0.2, 0.4, 0.6, 0.8, and 1.0. The ratio between the resistance and the stiffness of the vertical joints was taken as that of the self-tapping screw connections tested at FPIinnovations [4], i.e., 5.0.

Figures 22 and 23 show the relationship of the shear stiffness ratio to wall resistance and stiffness of the analysed balloon-type CLT shear walls. The ratios (Figures 22b and 23b) were based on the structural performance properties of the shear walls with the SSR of 0.01 and a given wall length. As shown in Figure 22, the resistance of 3 m and 6 m coupled walls increased with an increase in the SSR until 0.4 and 0.6, respectively, beyond which the resistance of the walls was governed by the hold-downs rather than the vertical joints. The stiffness of both wall configurations (Figure 23), increased dramatically when the SSR was less than 0.4, beyond that the increases became smaller. The relationship between the SSR and the  $L_c/L$  for analysed balloon-type walls is shown in Figure 24. The ratio  $L_c/L$  stayed constant for different SSRs, indicating that  $L_c/L$  of coupled shear walls is not affected by the SSR.

The deflection components of the coupled CLT shear walls with different SSRs were decoupled and the percentage of each component is shown in Figures 25 and 26. Bending, rotation, shear, and sliding deformation increased with an increase in the SSR, while the slip deflection decreased. Slip deflection was the major component for coupled walls with a small SSR, while bending deformation became the major component for coupled walls when the SSR was larger than 0.1.

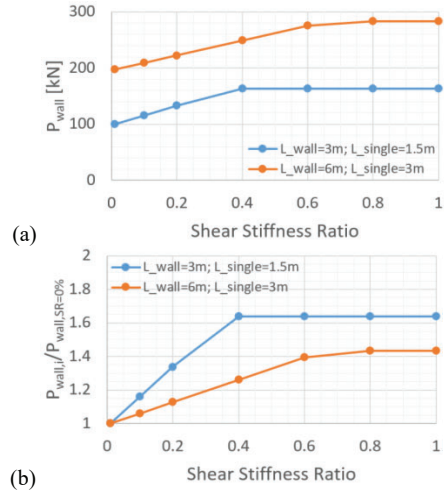


**Figure 22:** Relationship between SSR and wall resistance: (a) Absolute values; and (b) Relative values with respect to wall with SSR=0.01

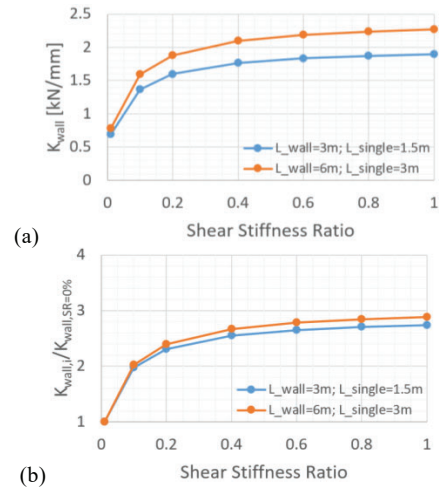


**Figure 23:** Relationship between SSR and wall stiffness: (a) Absolute values; and (b) Relative values with respect to wall with SSR=0.01

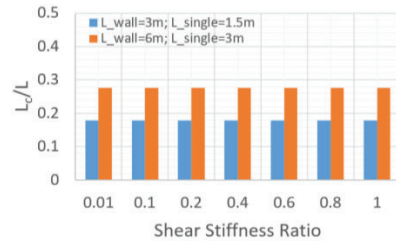


**Figure 24:** Relationship between shear stiffness ratio and compression length



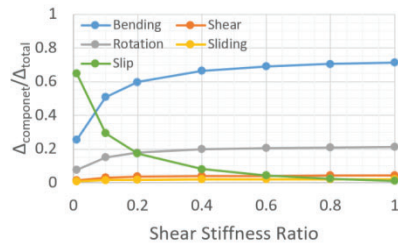


**Figure 25:** Influence of wall aspect ratio on the deflection components in 3.0 m coupled walls

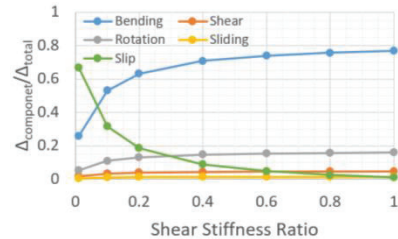


**Figure 26:** Influence of wall aspect ratio on the deflection components in 6.0 m coupled walls

## 4 CONCLUSIONS

A multi-year research project has been initiated at FPInnovations to quantify the system performance and develop the design information to codify balloon-type mass timber shear walls. A mechanics-based analytical model was updated to predict the CLT panel resistance, in addition to the deflection and resistance of balloon type CLT shear walls. Using this updated model, the influence of wall length and thickness, aspect ratio, vertical loads, and vertical joints on the seismic performance of this wall system was investigated. The findings are listed as follows:

- The lateral resistance and stiffness of balloon-type CLT shear walls increased with an increase in the wall length and thickness and decreased with an increase in the wall aspect ratio.
- The rotation and bending deflection were the two major contributors (e.g., 90% in total) to the total deflection of single panel balloon walls, while the shear deflection was the third one (e.g., 10%). The contribution of sliding was small enough to be ignored. As the wall aspect ratio increased, the walls became slender, and as a result the contribution of bending deflection increased (e.g., from 20% to 80%) and became the largest contributor to the total deflection, while the contribution of the rotation and the shear deflection decreased (e.g., rotational deflection changed from 80% to 20% and shear deflection changed from 10% to 1%).
- The lateral resistance and stiffness were affected by the vertical load level and the ratio of compression zone length to the wall length ( $L_c/L$ ). The resistance of walls increased with an increase in the vertical load level when  $L_c/L$  was either less than 0.4 or larger than

0.6, while it decreased with an increase in vertical load level when  $L_c/L$  was between 0.4 and 0.6. The stiffness of walls increased with vertical load level when  $L_c/L$  was less than 0.4 and decreased when  $L_c/L$  was larger than 0.4.

- The lateral resistance of 3 m and 6 m coupled walls increased with an increase in the shear stiffness ratio until 0.4 and 0.6, respectively, beyond which the resistance of the walls was governed by the hold-downs rather than the vertical joints. The stiffness of both wall configurations increased dramatically when the shear stiffness ratio was less than 0.4, beyond that the increase became smaller.
- In coupled balloon-type CLT shear walls, the bending, rotation, shear, and sliding deflection increased with an increase of the shear stiffness ratio, while the slip deflection decreased with increases in the shear stiffness ratio.

The updated analytical model will assist researchers and structural designers in developing and designing appropriate balloon-type CLT shear walls for timber structures. The analytical model can also be used to quantify the performance of balloon-type CLT structures subjected to seismic loads and thus providing the research background for drafting of the seismic design guidelines for balloon-type CLT construction for CSA O86 and National Building Code of Canada.

## ACKNOWLEDGEMENT

This project was financially supported by the Canadian Forest Service and National Resources Canada under the contribution agreement existing between the Government of Canada and FPInnovations.

## REFERENCES

- [1] Chen, Z., Popovski, M.: Mechanics-based analytical models for balloon-type cross-laminated timber (CLT) shear walls under lateral loads. *Engineering Structures*, 208:109916, 2020.
- [2] Izzi, M., Casagrande, D., Bezzi, S., Pasca, D., Follasa, M., and Tomasi, R.: Seismic behavior of Cross-Laminated Timber structures: A state-of-the-art review. *Eng. Struct.*, 170: 42-52, 2018.
- [3] Chen, Z., Popovski, M.: Expanding wood use towards 2025: Seismic performance of balloon mass timber walls – year 2. FPInnovations project report (301014059), Vancouver, 2021.
- [4] Chen, Z., Cuerrier-Auclair, S., and Popovski, M.: Advanced Wood-based Solutions for Mid-rise and High-rise Construction: Analytical Prediction Models for Balloon-Type CLT Shear Walls. FPInnovations Project Report (301012205), Vancouver, 2018.
- [5] Chen, Z., Tung, D., Karacabeyli, E.: Modelling Guide for Timber Structures. FPInnovations, 2022: [web.fpinnovations.ca/modelling](http://web.fpinnovations.ca/modelling)
- [6] Chen, Z., Popovski, M.: Modelling of mass timber seismic force resisting systems. FPInnovations, 2021.

- [7] Danielsson, H., & Serrano, E.: Cross laminated timber at in-plane beam loading – Prediction of shear stresses in crossing areas. *Eng. Struct.*, 171, 921-927, 2018.
- [8] Gavric, I., Fragiaco, M., & Ceccotti, A.: Cyclic Behavior of CLT Wall Systems: Experimental Tests and Analytical Prediction Models. *Journal of Structural Engineering*, 141(11): 04015034, 2015.
- [9] Blass, H. J., & Fellmoser, P.: Design of solid wood panels with cross layers. In: 8th World conf. timber eng. 2004.
- [10] Flaig, M., & Blass, H. J.: Shear strength and shear stiffness of CLT-beams loaded in plane. In: CIB-W18, 245-258, 2013.
- [11] CSA: Engineering design in wood (CSA O86:19). Canadian Standards Association (CSA), Toronto, 2019.
- [12] ANSI/APA: PRG 320 Standard for performance-rated cross-laminated timber. APA – The Engineered Wood Association, Tacoma, 2019.